Inorg. Chem. **2003**, *42*, 1475–1482

Flux Synthesis of the Noncentrosymmetric Cluster Compounds $Cs_2SnAs_2Q_9$ (Q = S, Se) Containing Two Different Polychalcoarsenite β-$[AsQ_4]^{3-}$ and $[AsQ_5]^{3-}$ Ligands

Ratnasabapathy G. Iyer, Junghwan Do, and Mercouri G. Kanatzidis*

Department of Chemistry and Center for Fundamental Materials Research, Michigan State University, East Lansing, Michigan 48824

Received October 1, 2002

Two noncentrosymmetric quaternary tin chalcoarsenates, $Cs_2SnAs_2S_9$ (**1**) and $Cs_2SnAs_2Se_9$ (**2**), were synthesized by the polychalcoarsenate flux method. Compound **1** crystallizes in the orthorhombic space group $Pmc2_1$ with a = 7.386(3) Å, b = 14.614(5) Å, c = 14.417(5) Å, and Z = 4. Compound **2** crystallizes in the monoclinic space group $P2_1$ with a = 7.715(5) Å, b = 17.56(1) Å, c = 7.663(5) Å, β = 115.86(1)°, and Z = 2. Both structures contain the same tin-centered molecular cluster anions $\{Sn[AsQ_2(Q_2)][AsQ(Q_2)_2]\}^{2-}$ (Q = S, Se) separated by Cs cations. The Sn^{4+} ion is in a distorted octahedral environment coordinated by two different pyramidal-shaped tridentate ligands, $[AsQ_2(Q_2)]^{3-}$ and $[AsQ(Q_2)_2]^{3-}$. These compounds absorb visible light at energies above 1.98 and 1.45 eV for **1** and **2**, respectively. Differential thermal analysis revealed that **1** melts at 350 °C and on cooling gives a glass. The glass recrystallizes at 268 °C upon subsequent heating. Compound **2** melts at 258 °C.

Introduction

Synthetic metal chalcoarsenates, although limited in number, present a variety of structures and anionic $[As_xQ_y]^{n-}$ (Q = S, Se) building units. Various $[As_xQ_y]^{n-}$ anions are known in ternary or quaternary compounds, with the pyramidal $[As^{III}Q_3]^{3-}$ and tetrahedral $[As^{V}Q_4]^{3-}$ being the most dominant.[1−4] Other examples include pyramidal $[As^{III}Q_4]^{3-}$ [5] and $[As^{III}Q_5]^{3-}$,[6] containing Q−Q bonds, and their condensed oligomeric forms such as $[As_2Q_5]^{4-}$, $[As_3Q_6]^{3-}$,[2b,d] and $[As_4Q_8]^{4-}$ [2a] anions. The number of naturally occurring thioarsenates is quite large, and this diversity is a harbinger of what could be expected in synthetically based systems. Structures with $[As^{III}Q_x]^{3-}$ (x = 3, 4, 5) units are expected to have unique structural chemistry because of the strong tendency of As^{3+} 4s lone pair to be stereochemically expressed. This property presents a dramatic distinction between chalcophosphate and chalcoarsenate chemistry despite the fact that P and As are in the same group. For example, corresponding analogues in chalcophosphates are seldom observed. Instead, the most stable oxidation states of P are 4+ and 5+ as found in the ethane-like $[P_2Q_6]^{4-}$ [7] and tetrahedral $[PQ_4]^{3-}$ [8] (Q = S, Se) ligands. This significant bifurcation in the chemistry of P and As and the desire to explore it are the main driving forces behind the work presented here.

To date, the hydro(solvento)thermal technique has been the primary means for the formation of ternary or quaternary

* To whom correspondence should be addressed. E-mail: kanatzid@cem.msu.edu.

(1) (a) Vater, V.; Sheldrick, W. S. *Z. Naturforsch., B* **1998**, *53*, 1259. (b) Cordier, G.; Schwidetzky, C.; Schäfer, H. *Z. Naturforsch., B* **1985**, *40*, 1. (c) Wachhold, M.; Sheldrick, W. S. *Z. Naturforsch., B* **1997**, *52*, 169. (d) Wachhold, M.; Sheldrick, W. S. *Z. Naturforsch., B* **1996**, *51*, 32.

(2) (a) Chou, J.-H.; Hanko, J. A.; Kanatzidis, M. G. *Inorg. Chem.* **1997**, *36*, 4. (b) Wachhold, M.; Kanatzidis, M. G. *Inorg. Chem.* **1999**, *38*, 4178. (c) Hanko, J. A.; Chou, J.-H.; Kanatzidis, M. G. *Inorg. Chem.* **1998**, *37*, 1670. (d) Chou, J.-H.; Kanatzidis, M. G. *Inorg. Chem.* **1994**, *33*, 1001. (e) Chou, J.-H.; Kanatzidis, M. G. *Inorg. Chem.* **1994**, *33*, 5372. (f) Wachhold, M.; Kanatzidis, M. G. *Inorg. Chem.* **2000**, *39*, 2337. (g) Chou, J.-H.; Kanatzidis, M. G. *J. Solid State Chem.* **1996**, *123*, 115. (h) Kanatzidis, M. G.; Chou, J.-H. *J. Solid State Chem.* **1996**, *127*, 186.

(3) (a) Jerome, J. E.; Wood, P. T.; Pennington, W. T.; Kolis, J. W. *Inorg. Chem.* **1994**, *33*, 1733. (b) O'Neal, S. C.; Pennington, W. T.; Kolis, J. W. *J. Am. Chem. Soc.* **1991**, *113*, 710. (c) O'Neal, S. C.; Pennington, W. T.; Kolis, J. W. *Inorg. Chem.* **1992**, *31*, 888.

(4) Pertlik F. *J. Solid State Chem.* **1994**, *112*, 170.

(5) Iyer, R. G.; Kanatzidis, M. G. *Inorg. Chem.* **2002**, *41*, *3605*.

(6) (a) McCarthy, T. J.; Hogan, T.; Kannewurf, C. R.; Kanatzidis, M. G. *Chem. Mater.* **1994**, *6*, 1072. (b) Hanko, J. A.; Sayettat, J.; Jobic, S.; Brec, R.; Kanatzidis, M. G. *Chem. Mater.* **1998**, *10*, 3040.

(7) (a) Chondroudis, K.; McCarthy, T. J.; Kanatzidis, M. G. *Inorg. Chem.* **1996**, *35*, 840. (b) Evenson, C. R.; Dorhout, P. K. *Inorg. Chem.* **2001**, *40*, 2884.

(8) (a) Aitken, J. A.; Canlas, C.; Weliky, D. P.; Kanatzidis, M. G. *Inorg. Chem.* **2001**, *40*, 6496. (b) Crystal data for $Cs_4As_2S_{10}$: monoclinic, $P2_1/c$; a = 17.669 Å, b = 7.1936 Å, c = 24.171 Å, β = 94.256°; R1 = 4.93%, wR2 = 9.19%.

10.1021/ic0260771 CCC: $25.00
Published on Web 02/01/2003

chalcoarsenate phases.[1,2] Depending on the counterion species, metal size, and pH employed in the reactions, a variety of chalcoarsenate anions are observed in the structures. However, little work exploring polychalcoarsenate fluxes has been reported. Recently, we have investigated the K/Sn/As/S system in such fluxes and obtained two thioarsenates, $KSnAsS_5$ and $K_2SnAs_2S_6$.[5] Whereas the rubidium chemistry gave only the isostructural analogues $RbSnAsS_5$ and $Rb_2SnAs_2S_6$, cesium chemistry gave different results.

Here, we report the synthesis, structures, and thermal and optical properties of two molecular tin chalcoarsenates, $Cs_2SnAs_2Q_9$ (Q = S, Se), prepared by polychalcoarsenate fluxes. Both compounds contain molecular tin-centered cluster anions $\{Sn[AsQ_2(Q_2)][AsQ(Q_2)_2]\}^{2-}$ (Q = S, Se) and adopt noncentrosymmetric polar space groups. An interesting property we discovered is the reversible crystal to glass transition of $Cs_2SnAs_2S_9$. Such transitions are of practical interest owing to potential applications in the field of optics.

Experimental Section

Reagents. The following reagents were used as obtained: Sn (99.999%; Cerac, Milwaukee, WI); As_2S_3 (99.9%; Strem Chemicals, Newburyport, MA); As (99.9%; Aldrich Chemical Co, Milwaukee, WI); S (99.9%; Strem Chemicals, Newburyport, MA); Se (99.999%; Noranda Advanced Materials, Quebec, Canada); *N*,*N*-dimethylformamide (Spectrum Chemicals, ACS reagent grade); diethyl ether. Cs_2S/Cs_2Se starting materials were prepared by a stoichiometric reaction of cesium metal and sulfur/selenium in liquid NH_3.

Synthesis. $Cs_2SnAs_2S_9$ (**1**) was synthesized from a mixture of 0.090 g (0.3 mmol) of Cs_2S, 0.018 g (0.15 mmol) of Sn, 0.037 g (0.15 mmol) of As_2S_3, and 0.048 g (1.5 mmol) of S. The reagents were mixed, sealed in an evacuated silica tube, and heated at 500 °C for 3 days and then cooled at a rate of 5 °C/h to 250 °C followed by rapid cooling to room temperature. The solid products were washed with *N*,*N*-dimethylformamide (DMF) and ether to remove the flux. Red plates and yellow irregular crystals (60/40% yield) were obtained. Electron microscope analysis of the crystals gave an average composition of $Cs_{2.1}SnAs_{1.9}S_{8.5}$ for the red plates and $Cs_{1.8}AsS_{4.9}$ for the yellow crystals. The yellow crystals, on single-crystal X-ray diffraction analysis, proved to be $Cs_4As_2S_{10}$, which is isostructural to $Cs_4P_2S_{10}$.[8] A single phase of **1** with over 95% yield was achieved by using a stoichiometric ratio of Cs_2S:Sn:As:S = 1:1:2:8 at 550 °C.

$Cs_2SnAs_2Se_9$ (**2**) was synthesized from a mixture of 0.172 g (0.5 mmol) of Cs_2Se, 0.059 g (0.5 mmol) of Sn, 0.112 g (1.5 mmol) of As, and 0.375 g (4.75 mmol) of Se. The reagents were mixed, sealed in an evacuated silica tube, and heated at 550 °C for 4 days. The tube was then cooled at a rate of 5 °C/h to 250 °C followed by rapid cooling to room temperature. The solid products were washed with *N*,*N*-dimethylformamide (DMF) and ether. Product recovery gave black platy single crystals of $Cs_2SnAs_2Se_9$ together with an unidentified glassy phase as indicated by X-ray powder diffraction. Quantitative synthesis of pure $Cs_2SnAs_2Se_9$ was achieved by a reaction of the stoichiometric amounts of Cs_2Se/Sn/As/Se at 500 °C. The product was stable in air and water. Electron microscope analysis of the crystals gave an average formula of "$Cs_2SnAs_2Se_{10}$". The structural details of the compounds were determined by a single-crystal X-ray diffraction study. Compounds **1** and **2** are soluble in polar solvents, such as *N*,*N*-dimethylformamide (DMF) and ethylenediamine, but insoluble in H_2O, acetone, and ethanol.

Physical Characterization Techniques

X-ray Powder Diffraction. Analyses were performed using a calibrated CPS 120 INEL X-ray powder diffractometer (Cu Kα radiation) operating at 40 kV/20 mA and equipped with a position-sensitive detector with a flat sample geometry.

Electron Microscopy. Semiquantitative analyses of the compounds were performed with a JEOL JSM-35C scanning electron microscope (SEM) equipped with a Tracor Northern energy dispersive spectroscopy (EDS) detector.

Solid-State UV/Vis and Infrared Spectroscopy. Optical diffuse reflectance measurements were performed at room temperature using a Shimadzu UV-3101 PC double-beam, double-monochromator spectrophotometer operating in the 200−2500 nm region using a procedure described in ref 2. Infrared spectra were recorded in the far-IR region (150−500 cm^{-1}) on a Nicolet 740 FT-IR spectrometer with a TSG/PE detector and silicon beam splitter using samples in the form of pressed CsI pellets.

Raman Spectroscopy. Raman spectra were recorded on a Holoprobe Raman spectrograph equipped with a CCD camera detector using 633 nm radiation from a HeNe laser for excitation and a resolution of 4 cm^{-1}. Laser power at the sample was estimated to be about 5 mW, and the focused laser beam diameter was ca. 10 μm. A total of 64 scans was sufficient to obtain good quality spectra.

Differential Thermal Analysis (DTA). DTA experiments were performed on Shimadzu DTA-50 thermal analyzer. Typically a sample (∼20 mg) of ground crystalline material was sealed in a silica ampule under vacuum. A similar ampule of equal mass filled with Al_2O_3 was sealed and placed on the reference side of the detector. Sample **1** was heated to 650 °C at 10 °C/min, and after 3 min it was cooled at a rate of −10 °C/min to 50 °C. A sample of **2** was heated to 600 °C using the same cycle as above. Residues of the DTA experiments were examined by X-ray powder diffraction. Reproducibility of the results was checked by running multiple heating/ cooling cycles.

X-ray Crystallography. The crystal structures of **1** and **2** were determined by single-crystal X-ray diffraction methods. Preliminary examination and data collection were performed on a SMART platform diffractometer equipped with a 1K CCD area detector using graphite-monochromatized Mo Kα radiation at room temperature. A hemisphere of data was collected using a narrow-frame method with scan widths of 0.30° in ω and an exposure time of 80 s/frame for **1** and 30 s/frame for **2**. The data were integrated using the SAINT program.[9] For **1** the program SADABS was used for the absorption correction, while an analytical absorption correction was employed for **2**. Additional crystallographic data for **1** and **2** are given in Table 1. In all cases satisfactory refinements were obtained with the noncentrosymmetric space groups, $Pmc2_1$ and $P2_1$ for **1** and **2**, respectively.

The initial positions for all atoms were obtained using direct methods, and the structures were refined by full-matrix least-squares techniques with the use of the SHELXTL crystallographic software package. After anisotropic refinement of all atom positions in **1**, there was one high-intensity peak remaining in the electron density map (5.35 e $Å^{-3}$). This peak (assigned as S13) was observed between the disulfide ion in the $[AsS(S_2)_2]^{3-}$ fragment and was 1.04 and 1.15 Å away from atoms S11 and S12, respectively. A disordered model was considered, and structure refinement led to 80% occupancy for S11 and S12 and 40% occupancy for S13, which resulted in drop of final R values from R1 = 0.0499 and

(9) *SAINT*, version 4.05; Siemens Analytical X-ray Instruments: Madison, WI, 1995.

Table 1. Crystallographic and Refinement Details for $Cs_2SnAs_2S_9$ and $Cs_2SnAs_2Se_9$

empirical formula	$Cs_2SnAs_2S_9$	$Cs_2SnAs_2Se_9$
fw	822.89	1244.99
space group	$Pmc2_1$ (No. 26)	$P2_1$ (No. 4)
a, Å	7.386(3)	7.175(5)
b, Å	14.614(5)	17.555(12)
c, Å	14.417(5)	7.663(5)
β, deg	90.0	115.857(11)
V, Å^3	1556.2(9)	868.5(11)
Z	4	2
cryst size, mm^3	0.19 × 0.19 × 0.09	0.15 × 0.08 × <0.01
ρ_{calcd}, g/cm^3	3.512	4.761
μ, cm^{-1}	282.08	116.43
T, K	296(2)	296(2)
λ, Å	0.71073	0.71073
θ range, deg	1.39−28.23	2.32−28.50
BASF	0.008(18)	0.17(7)
R1[a]	0.0399	0.0739
wR2[b]	0.1068	0.1442

[a] $R1 = \sum||F_o| - |F_c||/\sum|F_o|$. [b] $wR2 = \{\sum[w(F_o^2 - F_c^2)^2]/\sum[w(F_o^2)^2]\}^{1/2}$.

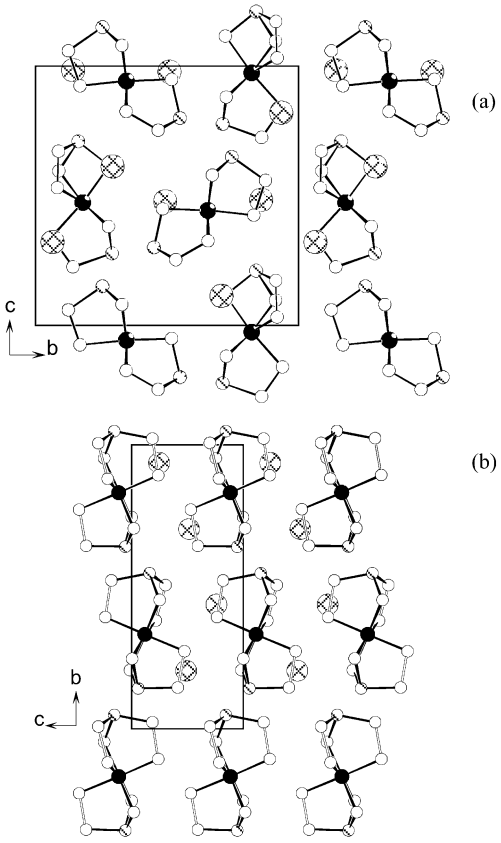

Figure 1. View of the unit cell of (a) **1** and (b) **2** along the *a* axis. Cesium, tin, arsenic, and selenium atoms are shown as crosshatched, black, hatched, and empty circles, respectively.

wR2 = 0.1369 to R1 = 0.0399 and wR2 = 0.1068. The remaining electron density peak/hole was 1.22/−1.21 eÅ^{-3}, found close to heavy atom positions (<1.01 Å). However, the structure refinement result considering the disordered disulfide ions does not give any reasonable structural models (d_{As-S13} = 2.432 Å, d_{Sn-S13} = 2.641 Å, $d_{S13-S13}$ = 2.886 Å). It is not clear why the disulfide ion in one cluster anion shows an unusual disorder. A possible supercell structure was sought; however, zone photos on the CCD diffractometer with long exposure times (5 min) gave no evidence for the presence of supercell reflections. The R values for the final cycle of the refinements based on F_o^2 are given in Table 1. The

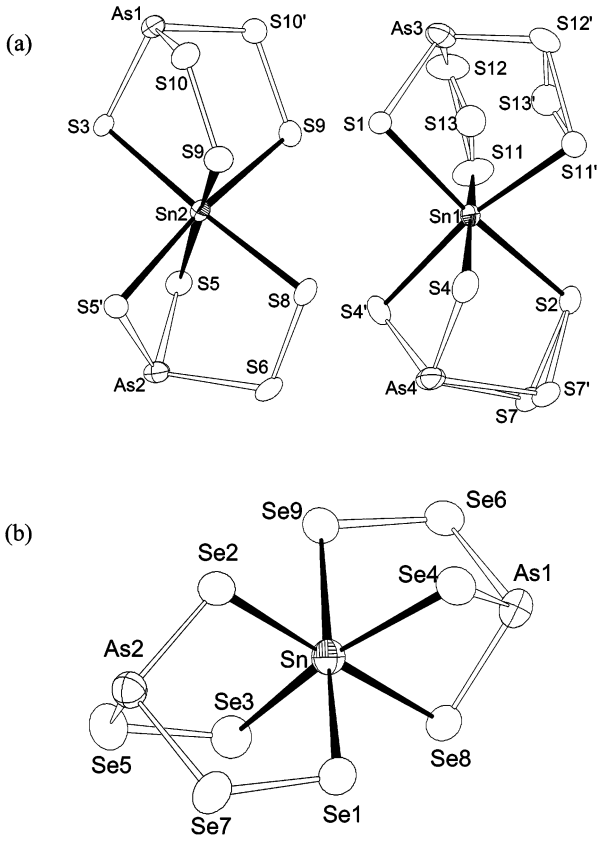

Figure 2. (a) The two crystallographically unique $[SnAs_2S_9]^{2-}$ anions in **1** and (b) the $[SnAs_2Se_9]^{2-}$ anion in **2**, with 30% thermal ellipsoids. Selected bond angles for **1** (deg): S11−Sn1−S11′ 98.4(2); S1−Sn1−S11 93.2(10); S4−Sn1−S4′ 79.56(15); S2−Sn1−S4 88.79(9); S1−Sn1−S2 174.20(12); S11−Sn1−S4 167.17(12); S3−Sn2−S9 91.70(8); S9−Sn2−S9′ 95.20(13); S5−Sn2−S5′ 79.14(12); S5−Sn2−S8 89.11(9); S3−Sn2−S8 175.87(12); S5−Sn2−S9 170.19(9); S3−As1−S10′ 100.13(9); S10−As1−S10′ 104.95(15); S5−As2−S6 98.28(10); S5−As2−S5′ 95.72(13); S1−As3−S12 103.57(13); S12−As3−S12′ 112.4(3); S4−As4−S7 103.64(16); S4−As4−S4′ 94.14(14). Selected bond angles for **2** (deg): Se1−Sn−Se2 91.4(3); Se2−Sn−Se3 95.7(3); Se3−Sn−Se1 91.3(3); Se4−Sn−Se8 79.8(3); Se8−Sn−Se9 95.5(3); Se4−Sn−Se9 84.0(2); Se3−Sn−Se4 165.4(3); Se2−Sn−Se8 178.3(3); Se1−Sn−Se9 173.2(3); Se6−As1−Se8 97.8(3); Se6−As1−Se4 101.4(3); Se4−As1−Se8 95.8(4); Se7−As2−Se5 103.7(4); Se2−As2−Se7 101.8(4); Se2−As2−Se5 102.1(4).

final R values for **1** are R1 = 0.0399 [$F_o^2 > 2\sigma(F_o^2)$] and wR2 = 0.1068 (all data). For **2**, the final R values are R1 = 0.0739 and wR2 = 0.1442 [$F_o^2 > 2\sigma(F_o^2)$].[10]

Results and Discussion

Synthesis. Compound **1** was prepared by using a flux ratio of 2:1:1:10 Cs_2S/Sn/As_2S_3/S at 500 °C. The influence of flux basicity on the reaction outcome was explored. A change in the flux basicity was achieved by altering the Cs_2S:S ratio. By increasing this ratio from 1:10 to 4:10 (i.e. increasing the basicity), we observed a substantial decrease in the sulfur content of the resulting compounds. For example, in the less basic sulfur-rich flux (1:10), a glassy red amorphous compound, with an average composition "$Cs_2SnAs_3S_{13}$" was

(10) Including all data for **2** the refinement parameters were quite high with R1 = 0.2744 and wR2 = 0.2332, which are indicative of poor quality of weak reflections. This may be caused by the very anisotropic morphology of the data crystal (0.15 × 0.08 × <0.01 mm^3).

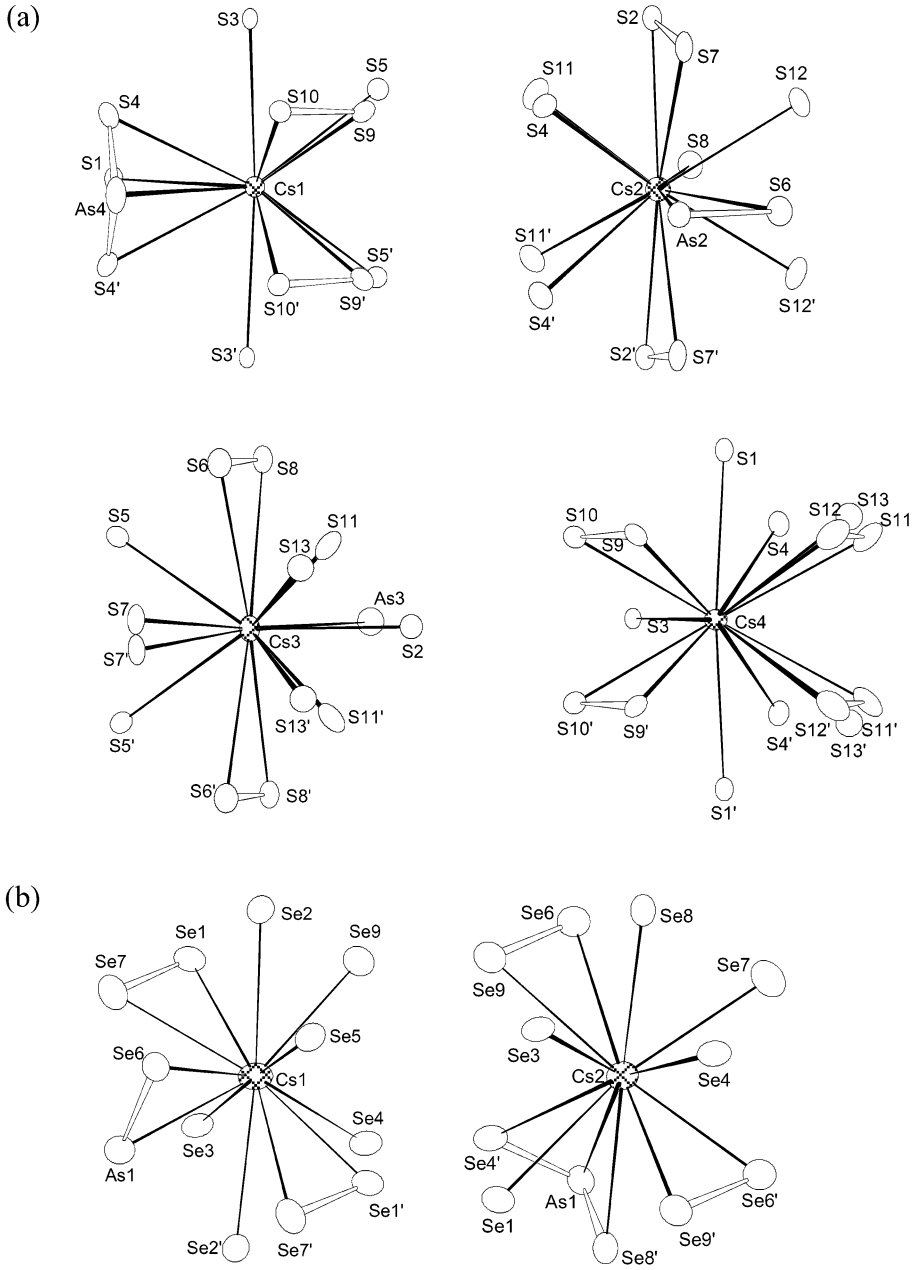

Figure 3. Local environments of Cs atoms in **1** (a) and **2** (b), with 30% thermal ellipsoids.

observed, whereas an orange flaky material "$Cs_3Sn_2AsS_7$" (average formula based on EDS) forms in a more basic but chalcogen-poor flux (4:10 Cs_2S/S). Assuming the compounds contain As^{3+} and Sn^{4+}, the former can be charge balanced with 2 S^{2-} + 5.5 S_2^{2-}, while the latter only with 7 S^{2-}. The title compound $Cs_2SnAs_2S_9$ (**1**), stabilized in ratio 2:10 Cs_2S/S, is charge balanced with 3 S^{2-} + 3 S_2^{2-}. Similar results were observed in the K/Sn/As/S system.[5]

In the selenide system, an alteration of the flux ratio also changed the reaction outcome but did not parallel the products in the sulfur system except for $Cs_2SnAs_2Se_9$ (**2**), which is a sulfur analogue and forms from a flux with 1:1:3:9.5 Cs_2Se/Sn/As/Se. By an increase of the ratio of Cs_2Se/Se from 1:9.5 to 3:9.5, the phase of **2** no longer forms. Instead the system phase-separates to produce Cs_3AsSe_4 and $Cs_4Sn_2Se_6$.

Structure. The crystal structure of $Cs_2SnAs_2S_9$ (**1**) was solved in the noncentrosymmetric space group $Pmc2_1$. The structure is built up of molecular complex anions $\{Sn[AsS_2(S_2)][AsS(S_2)_2]\}^{2-}$ separated by Cs^+ cations, Figure 1a. There are two crystallographically independent cluster anions in the unit cell of **1**. The Sn^{4+} ion is in a distorted octahedral environment coordinated by two pyramidal-shaped tridentate ligands, $[AsS_2(S_2)]^{3-}$ and $[AsS(S_2)_2]^{3-}$ forming a cagelike structure. The sulfur atom (S7) in the $[AsS_2(S_2)]^{3-}$ anion is disordered equally over two positions, Figure 2a. The Sn−S bond lengths range from 2.510(4) to 2.589(5) Å for Sn1 and 2.504(4) to 2.592(5) Å for Sn2, Figure 2.

Four crystallographically unique Cs^+ cations are surrounded by 11 S atoms in the range 3.628(3)−3.825(3) Å for Cs1, 3.557(4)−3.820(3) Å for Cs2, 3.478(5)−3.972(2) Å for Cs3, and 3.643(3)−3.756(5) Å for Cs4, Figure 3a.

Table 2. Selected Bond Lengths (Å) for $Cs_2SnAs_2S_9$ and $Cs_2SnAs_2Se_9$[a]

	$Cs_2SnAs_2S_9$		
Sn(1)−S(11)	2.510(3)	Sn(1)−S(11)$^{\#1}$	2.510(3)
Sn(1)−S(1)	2.520(3)	Sn(1)−S(4)$^{\#1}$	2.545(2)
Sn(1)−S(4)	2.545(2)	Sn(1)−S(2)	2.589(4)
Sn(1)−S(13)	2.641(8)	Sn(1)−S(13)$^{\#1}$	2.641(8)
Sn(2)−S(3)	2.504(3)	Sn(2)−S(9)	2.528(3)
Sn(2)−S(9)$^{\#4}$	2.528(3)	Sn(2)−S(5)$^{\#4}$	2.579(3)
Sn(2)−S(5)	2.579(3)	Sn(2)−S(8)	2.592(4)
As(1)−S(3)	2.194(4)	As(1)−S(10)$^{\#4}$	2.278(3)
As(1)−S(10)	2.278(3)		
As(2)−S(5)$^{\#1}$	2.216(3)	As(2)−S(5)$^{\#20}$	2.216(3)
As(2)−S(6)	2.304(4)		
As(3)−S(1)	2.190(3)	As(3)−S(12)	2.201(4)
As(3)−S(12)$^{\#1}$	2.201(4)	As(3)−S(13)	2.432(8)
As(3)−S(13)$^{\#1}$	2.432(8)		
As(4)−S(4)$^{\#1}$	2.224(3)	As(4)−S(4)	2.224(3)
As(4)−S(7)$^{\#1}$	2.328(5)	As(4)−S(7)	2.328(5)
S(2)−S(7)$^{\#1}$	2.049(7)	S(6)−S(8)$^{\#12}$	2.046(6)
Cs(1)−S(5)$^{\#6}$	3.628(3)	Cs(1)−S(5)$^{\#4}$	3.628(3)
Cs(1)−S(1)	3.679(3)	Cs(1)−S(3)	3.7225(13)
Cs(1)−S(3)$^{\#6}$	3.7225(13)	Cs(1)−S(9)$^{\#6}$	3.752(3)
Cs(1)−S(9)$^{\#4}$	3.752(3)	Cs(1)−S(4)	3.820(3)
Cs(1)−S(4)$^{\#1}$	3.820(3)	Cs(1)−S(10)$^{\#4}$	3.825(3)
Cs(1)−S(10)$^{\#6}$	3.825(3)	Cs(1)−As(4)	4.145(2)
Cs(2)−S(11)$^{\#7}$	3.557(4)	Cs(2)−S(11)$^{\#8}$	3.557(4)
Cs(2)−S(12)$^{\#9}$	3.589(4)	Cs(2)−S(12)$^{\#10}$	3.589(4)
Cs(2)−As(2)$^{\#8}$	3.7038(18)	Cs(2)−S(2)$^{\#11}$	3.7043(13)
Cs(2)−S(2)$^{\#8}$	3.7043(13)	Cs(2)−S(8)$^{\#12}$	3.732(4)
Cs(2)−S(7)$^{\#1}$	3.792(6)	Cs(2)−S(7)$^{\#11}$	3.792(6)
Cs(2)−S(4)$^{\#8}$	3.820(3)	Cs(2)−S(4)$^{\#7}$	3.820(3)
Cs(3)−S(7)$^{\#3}$	3.478(5)	Cs(3)−S(7)$^{\#14}$	3.478(5)
Cs(3)−S(2)$^{\#15}$	3.628(4)	Cs(3)−S(5)$^{\#16}$	3.678(3)
Cs(3)−S(5)$^{\#17}$	3.678(3)	Cs(3)−S(8)$^{\#17}$	3.8185(16)
Cs(3)−S(8)$^{\#18}$	3.8185(16)	Cs(3)−S(11)$^{\#19}$	3.841(5)
Cs(3)−S(11)$^{\#15}$	3.841(5)	Cs(3)−S(6)$^{\#2}$	3.8492(17)
Cs(3)−S(6)$^{\#3}$	3.8492(17)	Cs(3)−As(3)	3.972(2)
Cs(4)−S(3)$^{\#10}$	3.643(3)	Cs(4)−S(12)$^{\#9}$	3.655(5)
Cs(4)−S(12)$^{\#10}$	3.655(5)	Cs(4)−S(9)$^{\#12}$	3.658(3)
Cs(4)−S(9)$^{\#20}$	3.658(3)	Cs(4)−S(1)$^{\#21}$	3.6995(13)
Cs(4)−S(1)$^{\#10}$	3.6995(13)	Cs(4)−S(10)$^{\#12}$	3.707(3)
Cs(4)−S(10)$^{\#20}$	3.707(3)	Cs(4)−S(11)$^{\#9}$	3.756(5)
Cs(4)−S(11)$^{\#10}$	3.756(5)	Cs(4)−S(13)$^{\#9}$	3.762(8)
	$Cs_2SnAs_2Se_9$		
Sn−Se(3)	2.670(7)	Sn−Se(2)$^{\#2}$	2.672(8)
Sn−Se(1)	2.686(8)	Sn−Se(8)	2.691(8)
Sn−Se(9)$^{\#2}$	2.707(8)	Sn−Se(4)	2.749(8)
As(1)−Se(4)$^{\#8}$	2.323(10)	As(1)−Se(8)$^{\#8}$	2.380(10)
As(1)−Se(6)	2.444(9)		
As(2)−Se(2)$^{\#2}$	2.300(10)	As(2)−Se(5)$^{\#9}$	2.406(9)
As(2)−Se(7)	2.416(10)		
Se(1)−Se(7)	2.306(12)	Se(3)−Se(5)$^{\#9}$	2.308(11)
Se(6)−Se(9)$^{\#10}$	2.293(11)		
Cs(1)−Se(1)	3.615(8)	Cs(1)−Se(3)$^{\#1}$	3.622(8)
Cs(1)−Se(9)$^{\#1}$	3.643(9)	Cs(1)−Se(1)$^{\#1}$	3.719(8)
Cs(1)−Se(5)	3.767(10)	Cs(1)−Se(7)$^{\#1}$	3.772(9)
Cs(1)−Se(6)	3.828(9)	Cs(1)−As(1)	3.840(10)
Cs(1)−Se(4)	3.916(9)	Cs(1)−Se(2)$^{\#2}$	3.944(7)
Cs(1)−Se(2)$^{\#1}$	3.970(7)	Cs(1)−Se(7)	4.055(9)
Cs(2)−Se(3)$^{\#3}$	3.678(9)	Cs(2)−Se(6)$^{\#4}$	3.717(7)
Cs(2)−Se(9)	3.771(8)	Cs(2)−Se(7)$^{\#4}$	3.807(9)
Cs(2)−Se(9)$^{\#1}$	3.809(8)	Cs(2)−Se(6)$^{\#5}$	3.825(7)
Cs(2)−Se(4)	3.885(8)	Cs(2)−Se(8)$^{\#3}$	3.920(7)
Cs(2)−Se(4)$^{\#6}$	3.944(8)	Cs(2)−Se(1)	3.966(9)
Cs(2)−Se(8)	3.973(7)	Cs(2)−As(1)$^{\#7}$	4.077(8)

[a] Symmetry transformations used to generate equivalent atoms are as follows. $Cs_2SnAs_2S_9$: #1, $-x+1, y, z$; #2, $x+1, y, z+1$; #3, $x, y, z+1$; #4, $-x, y, z$; #5, $x-1, y, z$; #6, $x+1, y, z$; #7, $x, -y, z-\times$ba; #8, $-x, -y, z-\times$ba; #9, $-x, y, z-1$; #10, $x, y, z-1$; #11, $-x+1, -y, z-\times$ba; #12, $-x, -y+1, z-1/2$; #13, $x-1, -y, z-1/2$; #14, $-x+1, y, z+1$; #15, $-x+1, -y, z+1/2$; #16, $x+1, -y+1, z+1/2$; #17, $-x, -y+1, z+1/2$; #18, $-x+1, -y+1, z+1/2$; #19, $x, -y, z+1/2$; #20, $x, -y+1, z-1/2$; #21, $x-1, y, z-1$. $Cs_2SnAs_2Se_9$: #1, $x+1, y, z$; #2, $x, y, z-1$; #3, $x+1, y, z+1$; #4, $-x+2, y-1/2, -z+1$; #5, $-x+3, y-1/2, -z+1$; #6, $x, y, z+1$; #7, $-x+2, y-1/2, -z$; #8, $-x+2, y+1/2, -z$; #9, $x-1, y, z-1$; #10, $-x+2, y+1/2, -z+1$.

There are several weak interactions of Cs1, Cs2, and Cs3 with As4, As2, and As3, respectively, at distances of 4.145, 3.703, and 3.976 Å. The average S−S distance is normal at 2.0475 Å, Table 2. A similar unusual interaction between the K^+ ion and As atom was observed in $K_2SnAs_2S_6$.[5]

The crystal structure of $Cs_2SnAs_2Se_9$ (**2**) was solved in the polar space group $P2_1$ and contains the same structural motif as **1,** i.e., $\{Sn[AsS_2(Se_2)][AsS(Se_2)_2]\}^{2-}$ cluster anions. However, the unit cell of **2** contains only one crystallographically unique cluster anion and no disorder, Figure 1b. The octahedral Sn center has Sn−Se bond distances ranging from 2.670(7) Å to 2.750(8) Å. All the Sn−Se, As−Se, and Se−Se distances and angles are normal; see Table 2. Two crystallographically unique Cs^+ cations are 12-coordinated by 11 Se and 1 As atoms in the range 3.615(8)−4.055(9) Å for Cs1 and 3.678(9)−4.077(8)Å for Cs2, Figure 3b. Weak interactions are also observed in **2** at 3.84(1) and 4.077(8) Å between $Cs1^+$ and $Cs2^+$ ions and the As1 atom. Selected bond lengths for **1** and **2** are given in Table 2.

A salient structural feature of these compounds is the presence of two different chalcoarsenate ligands. The pyramidal anions $[AsQ_2(Q_2)]^{3-}$ and $[AsQ(Q_2)_2]^{3-}$ contain one and two dichalcogenide units, respectively. In previous work, we found $[AsS_2(S_2)]^{3-}$ in the chain compound $KSnAsS_5$.[5] However, this is the first time that $[AsS(S_2)_2]^{3-}$ and $[AsSe_2(Se_2)]^{3-}$ and $[AsSe(Se_2)_2]^{3-}$ have been isolated in such fluxes.

The structure of the double cagelike $[SnAs_2Q_9]^{2-}$ cluster anion is reminiscent of those in the centrosymmetric compounds $[(n\text{-}Bu)_4N]_2[MAs_2Se_{10}]$[3c] (M = Mo, W), which also have two $[AsSe(Se_2)_2]^{3-}$ ligands. There are unusually short Se−Se distances between two cages, 2.702 Å for Mo and 2.708 Å for W in $[M(AsSe_5)_2]^{2-}$ (M = Mo, W). This shortening is caused by electron transfer from the Se atoms to Mo^{4+} (or W^{4+}) centers. Given that such a transfer is not likely in Sn^{4+}, no unusual Q−Q distances are found or expected in **1** and **2**. All nonbonded Q−Q distances between the two cages are longer at 3.380 and 3.621 Å for **1** and **2**, respectively.

An important feature of the flux method is the freedom it allows the metal to choose it own ligands for lattice construction. In this context, an issue that deserves comment is the composition of the cluster anion, $[SnAs_2Q_9]^{2-}$, which contains both $[AsQ_5]^{3-}$ and $[AsQ_4]^{3-}$ instead of only one type of ligand. A speculative explanation of this behavior can be based on electronic and steric considerations of the ligands involved. $[AsQ_5]^{3-}$ being more electron donating than $[AsQ_4]^{3-}$, because of the additional chalcogen atom, coupled with its ability to form a larger cage, might be preferred by the electrophilic Sn^{4+} ion. Coordination to this ligand reduces the electron density requirement of the central metal atom and allows for the relatively less electron rich and less bulky $[AsQ_4]^{3-}$ to bind.

Thermal Analysis. Differential thermal analysis of $Cs_2SnAs_2S_9$ showed that it melts at 350 °C with no recrystallization observed on cooling, instead giving a glass product, Figure 4a. The glass has the same red color as crystalline $Cs_2SnAs_2S_9$. The X-ray powder pattern of the material at the end of the DTA cycle confirms its noncrystalline nature.

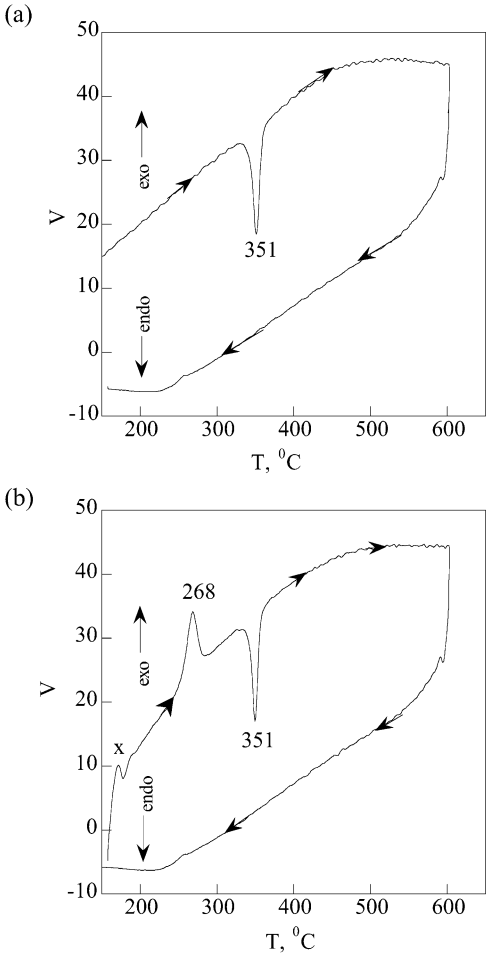

Figure 4. Differential thermal analysis plots of **1** showing (a) melting in the first cycle with no recrystallization upon cooling and (b) subsequent recrystallization (exothermic peak at 268 °C) on heating in the second cycle. The peak marked "x" is an instrumental artifact.

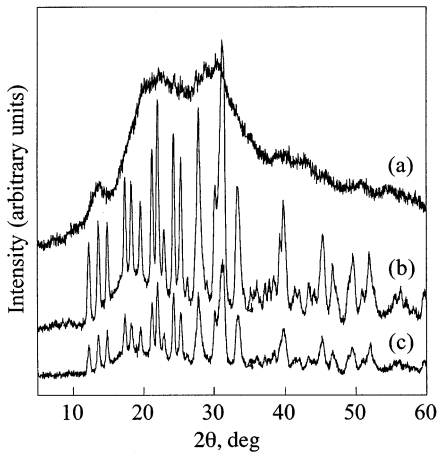

Figure 5. X-ray diffraction patterns of (a) glassy $Cs_2SnAs_2S_9$, (b) pristine $Cs_2SnAs_2S_9$, and (c) recrystallized $Cs_2SnAs_2S_9$.

The glass recrystallizes exothermically at 268 °C upon subsequent heating (Figure 4b). The powder pattern taken after the recrystallization matches the one taken before the start of the experiment and indicates no decomposition, Figure 5. It is noteworthy that reversible glass/crystal phase changes of this type are of great interest in optical storage applications and the field of optics.[11]

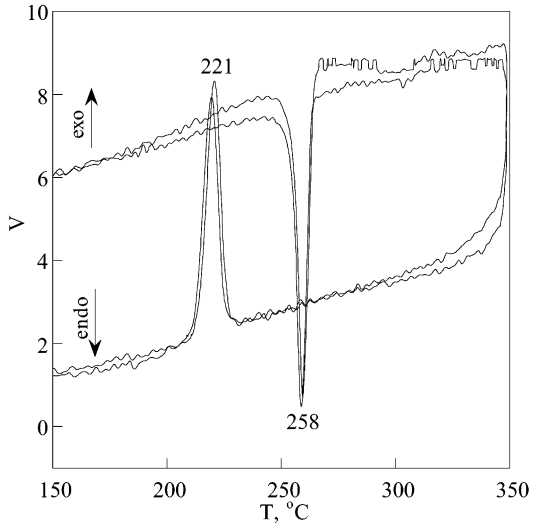

Figure 6. Differential thermal analysis of **2** showing a melting point of 258 °C and a recrystallization point of 221 °C.

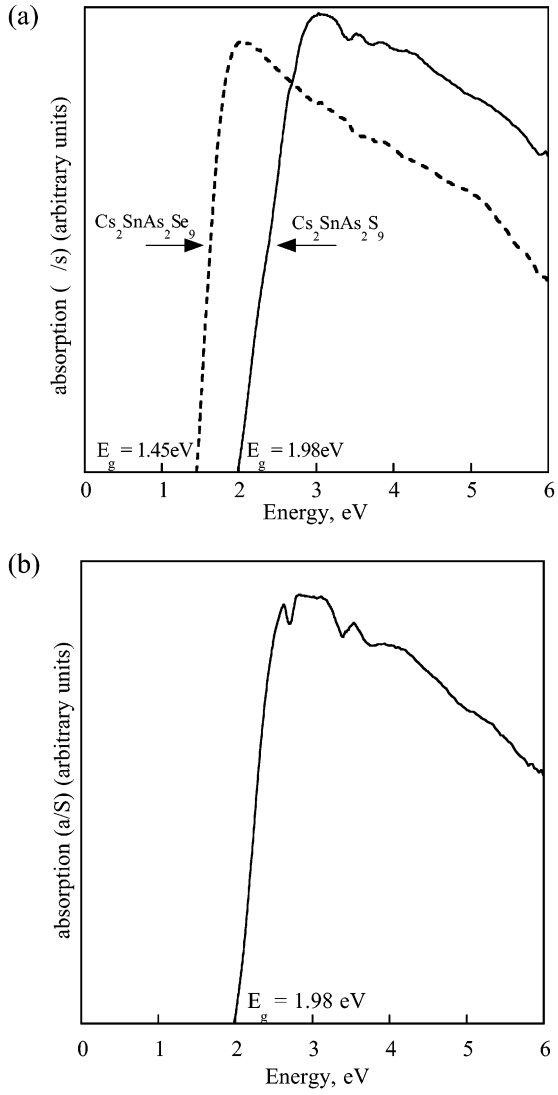

Figure 7. Optical absorption spectra showing absorption edges at (a) 1.98 eV for **1** (solid line) and 1.45 eV for **2** (dotted line) and (b) 1.98 eV for the glass of **1**.

$Cs_2SnAs_2Se_9$, on subjecting to the same heating/cooling rate as above, melts at ~258 °C and partially crystallizes at

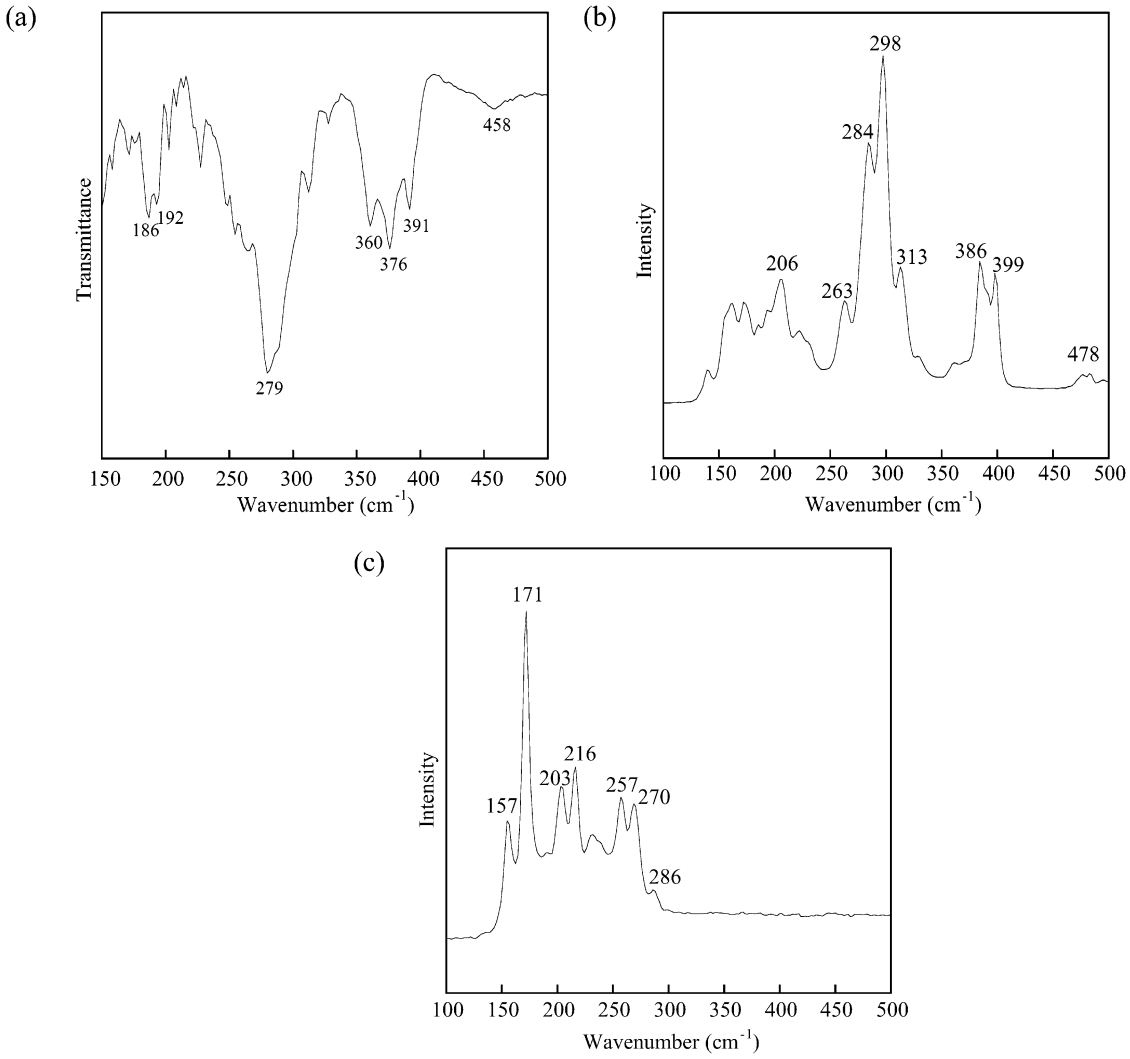

Figure 8. (a) Far-IR of **1**, (b) Raman spectrum of **1**, and (c) Raman spectrum of **2**. The peak at 478 cm^{-1} in the Raman spectrum of **1** is due to S−S stretching.

200 °C. Complete recrystallization occurs in the second cycle on heating at 220 °C. Therefore, a slower cooling rate of 2 °C/min was employed which revealed that the compound melts congruently at ∼258 °C and recrystallizes at 221 °C, Figure 6. The thermal behavior of $Cs_2SnAs_2Se_9$ suggests that it could be converted to a glass if more rapid cooling were used, e.g. >10 °C/min.

Spectroscopy. The solid-state diffuse reflectance UV/vis spectra of **1** and **2** revealed steep absorption edges corresponding to band gaps of 1.98 and 1.45 eV, respectively, which are consistent with their red and black colors, Figure 7. The reddish glass product of **1** after the DTA cycle also shows a band gap of 1.98 eV. Given the discrete molecular nature of the anions in **1** and **2**, it is not clear whether a band description is appropriate here for the electronic structure of these materials. The observed electronic absorptions are most probably local (i.e. intracluster) in nature, and thus, they correspond to HOMO−LUMO gaps.[12] The absence of the typical red shift in the absorption edge, as it is typically observed in the glassy forms of compounds with extended solid-state structures,[13] also supports the notion that the electronic properties of **1** and **2** are local (intracluster) in nature. In extended systems with a well-developed band structure the crystal to glass conversion produces a red shift because of the large number of defect-induced midgap states generated in the glass. The discrete molecular structure of $Cs_2SnAs_2S_9$ does not generate such states, and the glass structure probably represents a disordered arrangement of discrete $[SnAs_2S_9]^{2-}$ anions and Cs^+ cations.

The far-IR spectra display peaks at 391 (s), 376 (s), 360 (s), 328 (m), 312 (m), 279 (s), 265 (w), 254 (m), 247 (w), 227 (s), 213 (w), 208 (m), 203 (s), 192 (w), 186 (m), 171 (m) cm^{-1} for **1**, Figure 8a, and 412 (w), 402 (w), 390 (w), 379 (w), 345 (w), 332 (m), 320 (m), 308 (m), 294 (m-s),

(11) (a) Yamada, N.; Ohno, E.; Nishiuchi, K.; Akahira, N.; Takao, M. *J. Appl. Phys.* **1991**, *69* (5), 2849−2856. (b) Rubin, K. A.; Birnie, D. P.; Chen, M. *J. Appl. Phys.* **1992**, *71* (8), 3680−3687. (c) Ohta, T. *J. Optoelec. Adv. Mater.* **2001**, *3* (3), 609−626. (d) Yamada, N.; Matsunaga, T. *J. Appl. Phys.* **2000**, *88* (12), 7020−7028.

(12) Definitions: HOMO, highest occupied molecular orbital; LUMO, lowest unoccupied molecular orbital.

(13) (a) Dhingra, S.; Kanatzidis, M. G. *Science* **1992**, *258*, 1769. (b) Marking, G. A.; Hanko, J. A.; Kanatzidis, M. G. *Chem. Mater*. **1998**, *10*, 1191.

271 (s), 260 (s), 251 (m-s), 235 (s), 219 (s), 207 (s), 190 (m), 185 (m-s), 165 (s) cm^{-1} for **2**. On the basis of previous reports,[14] the peaks in **1** from 400 to 310 cm^{-1} can be assigned to As−S stretching vibrations. These vibrations appear at a lower energy from 250 to 200 cm^{-1} in the case of **2**. The peaks at lower wavenumbers can be attributed to Sn−Q stretching or As−Q bending modes. The Raman spectrum of **1** shows peaks at 478, 399, 386, 313, 298, 284, and 263 cm^{-1}, Figure 8b. Again these could be due to Sn−S or As−S vibrations. On the basis of the Raman spectra of polysulfides, the peak at 478 cm^{-1} is assigned to the S−S stretching vibration. Raman shifts at 157, 171, 203, 216, 232, 257, 270, and 286 cm^{-1} are observed for **2**, Figure 8c.

In conclusion, cesium polychalcoarsenate fluxes allowed the discovery of two novel compounds, $Cs_2SnAs_2Q_9$ (Q = S, Se), containing discrete cluster molecules. Their noncentrosymmetric space groups, a requisite condition to observe nonlinear optical second harmonic generation, make them interesting candidates for detailed nonlinear optical investigations. In addition, the glass formation ability of $Cs_2SnAs_2S_9$ and $Cs_2SnAs_2Se_9$ is an intriguing property that requires further scrutiny for exploring optical data storage applications.

Acknowledgment. Financial support from the National Science Foundation (Grant DMR-0127644) is gratefully acknowledged.

Supporting Information Available: Tables of crystallographic details, atomic coordinates, isotropic and anisotropic displacement parameters for all atoms, and interatomic distances and angles for $Cs_2SnAs_2S_9$ and $Cs_2SnAs_2Se_9$, in CIF format. This material is available free of charge via the Internet at http://pubs.acs.org.

IC0260771

(14) (a) Bastow, T. J.; Whitfield, H. J. *J. Chem. Soc., Dalton Trans*. **1973**, 1739. (b) Billes, F.; Mitsa, V.; Mateleshko, N.; Fejsa, I. *J. Mol. Struct.* **1999**, *513*, 109. (c) Nakamoto, K. *Infrared and Raman Spectra of Inorganic and Coordination Compounds*, 5th ed.; John Wiley and Sons: New York, 1997.